



Naafs, D., & Pancost, R. (2016). Sea-surface temperature evolution across Aptian Oceanic Anoxic Event 1a. *Geology*, 44(11), 959-962. <https://doi.org/10.1130/G38575.1>

Peer reviewed version

Link to published version (if available):  
[10.1130/G38575.1](https://doi.org/10.1130/G38575.1)

[Link to publication record in Explore Bristol Research](#)  
PDF-document

This is the accepted author manuscript (AAM). The final published version (version of record) is available online via Geological Society of America at <http://dx.doi.org/10.1130/G38575.1>. Please refer to any applicable terms of use of the publisher.

## University of Bristol - Explore Bristol Research

### General rights

This document is made available in accordance with publisher policies. Please cite only the published version using the reference above. Full terms of use are available: <http://www.bristol.ac.uk/red/research-policy/pure/user-guides/ebr-terms/>

# 1 Sea surface temperature evolution across Aptian Oceanic 2 Anoxic Event 1a

3  
4 **B.D.A. Naafs\* and R.D. Pancost**

5  
6 Organic Geochemistry Unit, School of Chemistry and Cabot Institute, University of  
7 Bristol, BS8 1TS Bristol, UK

8  
9 \*Corresponding author. E-mail address: [david.naafs@bristol.ac.uk](mailto:david.naafs@bristol.ac.uk)

## 10 11 **ABSTRACT**

12 Atmospheric CO<sub>2</sub> possibly doubled during Oceanic Anoxic Event (OAE) 1a, likely in  
13 response to submarine volcanic outgassing. Despite being important for our  
14 understanding of the consequences of carbon cycle perturbations, the response of the  
15 climate system to this increase in greenhouse forcing is poorly constrained. Here we  
16 provide a new sea surface temperature (SST) record from the mid-latitude proto-  
17 North Atlantic based on the organic geochemical TEX<sub>86</sub>-paleothermometer. Using  
18 different calibrations, including the newly developed BAYSPAR deep time analogue  
19 approach, we demonstrate that SSTs increased by ~ 2-4 °C during OAE 1a and  
20 decreased by ~ 4-6 °C at its end, both simultaneous with changes in  $\delta^{13}\text{C}_{\text{org}}$ , which we  
21 argue reflects changes in  $p\text{CO}_2$ . We demonstrate that a clear latitudinal SST-gradient  
22 prevailed during OAE 1a, contrary to the generally accepted view that a nearly flat  
23 SST-gradient existed during OAE 1a and the Early Cretaceous. These results are more

consistent with climate model simulations of the Cretaceous that have failed to produce flat SST-gradients.

## INTRODUCTION

The Aptian Oceanic Anoxic Event (OAE) 1a, ~ 120 million years ago (Myr), is characterized by large perturbations of the global carbon cycle. New high-resolution records demonstrate that  $p\text{CO}_2$  increased, potentially doubling, during the first part of OAE 1a and after 1.5-2 million years returned to pre-event values (Naafs et al., 2016). However the responses of the climate system to these changes in greenhouse forcing are poorly constrained, representing a fundamental gap in our understanding of this OAE.

Sea surface temperatures (SSTs) are one of the most diagnostic features of climate and frequently used to constrain climate model simulations. However, many OAE 1a sections are characterized by large changes in sedimentology and (partial) disappearance of biogenic carbonates. Combined with the absence of suitable foraminifera in (most) Early Cretaceous sediments, SST change during OAE 1a has generally been inferred from bulk  $\delta^{18}\text{O}$  values (e.g., Ando et al., 2008). However these values are susceptible to diagenesis (Jenkyns, 1995), and the correlation between  $\delta^{18}\text{O}$  and SST depends on sea water chemistry such as  $\delta^{18}\text{O}_{\text{sw}}$  and pH (e.g., Ando et al., 2008), which are poorly constrained for the Early Cretaceous but was likely different from the modern (e.g., Ridgwell, 2005).

The organic palaeothermometer  $\text{TEX}_{86}$  is increasingly used to reconstruct SSTs during the Cretaceous.  $\text{TEX}_{86}$  is based on the empirical relationship in the modern ocean between the distribution of marine archaeal membrane lipids (GDGTs) in the core tops of marine sediments and overlying SSTs (Schouten et al., 2002).

TEX<sub>86</sub> is also susceptible to a number of caveats that must be considered in its application; for example it can potentially be affected by changes in oxygen availability (Qin et al., 2015), and there is uncertainty regarding the exact production depth of the sedimentary TEX<sub>86</sub> signal (Taylor et al., 2013). However, TEX<sub>86</sub> does not appear to be systematically influenced by diagenesis (Huguet et al., 2009) nor changes in sea water chemistry such as salinity and pH (Elling et al., 2015). As such TEX<sub>86</sub> can be used to provide complementary and new Mesozoic SST records, especially during periods with poor carbonate preservation.

The available TEX<sub>86</sub> records either do not span the entire  $\delta^{13}\text{C}$  perturbation (Dumitrescu et al., 2006), have relatively poor temporal resolution (Jenkyns et al., 2012; Mutterlose et al., 2014; Schouten et al., 2003) and/or are influenced by thermal maturity (Bottini et al., 2015). Here we provide the first high-resolution TEX<sub>86</sub>-based SST record spanning OAE 1a from the astronomically tuned record of deep sea drilling project (DSDP) Site 398 in the mid-latitude proto-North Atlantic to infer the SST evolution across OAE 1a and we compare that to other TEX<sub>86</sub> records to explore global SST patterns.

## **DSDP SITE 398**

At Site 398 OAE 1a spans about 20 m, between 1571.26 and 1550.77 meters below the sea floor (mbsf) and representing ~ 1.3 million year (Myr) (Li et al., 2008). Our record ranges from 1590 to 1535 mbsf (or ~ 3.5 Myr) and covers the characteristic negative (isotope segment C3) and subsequent positive carbon isotope excursion (CIE) across carbon isotope segments C4-C7 (Menegatti et al., 1998) although these individual segments can't all be distinguished at Site 398 (Li et al., 2008). These variations in  $\delta^{13}\text{C}$  have been observed globally and reflect large perturbations of the

global carbon cycle and changes in  $p\text{CO}_2$  (Naafs et al., 2016). The organic matter at Site 398 is thermally immature (Naafs et al., 2016) and the lithology remains relatively constant across OAE 1a, consisting of calcareous claystone and mudstone (Li et al., 2008).

## **ANALYTICAL METHODS**

For this study we analysed 40 samples from DSDP Site 398, as well as five samples from the Djebel Serdj FM in Tunisia. Lipids from Site 398 were obtained by extracting sediment with an Ethos Ex microwave extraction system, whereas the samples from the Djebel Serdj were extracted using Soxhlet apparatus for 24 hr (see supplementary information). The total lipid extract was separated into different fractions and the polar fractions (containing the GDGTs) were re-dissolved in hexane/iso-propanol (99:1, v/v) and passed through a 0.45  $\mu\text{m}$  PTFE filter prior to analysis by a ThermoFisher Scientific Accela Quantum Access triple quadrupole mass spectrometer instrument.

## **CHOICE OF $\text{TEX}_{86}$ CALIBRATION**

Previous OAE 1a studies have used the widely applied  $\text{TEX}_{86}^{\text{H}}$ -calibration (Kim et al., 2010) to translate  $\text{TEX}_{86}$  values into SSTs.  $\text{TEX}_{86}^{\text{H}}$  assumes a logarithmic relationship between core top  $\text{TEX}_{86}$  values and overlying mean annual SST. However, there is no evidence for a logarithmic relationship between  $\text{TEX}_{86}$  and SSTs, the modern latitudinal temperature gradient of  $\text{TEX}_{86}^{\text{H}}$ -based SSTs is reduced compared to the instrumental record, and  $\text{TEX}_{86}^{\text{H}}$  is characterized by structured residual trends that bias SST reconstructions, especially outside the modern calibration range (Tierney and Tingley, 2014, 2015). The consequences are that

TEX<sub>86</sub><sup>H</sup> yields a maximum possible SST of 39 °C and exhibits a dampened SST sensitivity at TEX<sub>86</sub> values higher than those found in the modern tropics (about 0.8), likely underestimating absolute SSTs estimates but also the amplitude of spatial and temporal trends. Other global TEX<sub>86</sub> calibrations have assumed a linear relationship (Schouten et al., 2002). A linear relationship (even at high temperatures) is supported by incubation and mesocom experiments that demonstrate that the temperature dependence of TEX<sub>86</sub> remains linear at temperatures as high as 40 °C (Schouten et al., 2007).

In the context of the above mentioned complications and lack of evidence for a logarithmic calibration, we applied the deep time analogue approach of BAYSPAR (Tierney and Tingley, 2014) to our new data and all previously generated TEX<sub>86</sub> data for OAE 1a. The deep time analogue approach assumes a linear temperature dependence of TEX<sub>86</sub>, but treats the intercept and slope of the linear regression as independent Gaussian processes that can vary depending on the modern analogues used to define the deep time calibration (see Supplementary Information).

## RESULTS

All but 3 samples from Site 398 contained sufficient GDGTs to calculate TEX<sub>86</sub> values. The BIT-index, which reflects the relative contribution of terrestrial versus marine GDGTs (Hopmans et al., 2004), is generally below 0.4 with an average value of 0.2, mitigating concerns regarding the contribution of terrestrial-derived GDGTs. Five samples had BIT indices between 0.41 and 0.57 and although these data points are shown in figure 1, they are not used to calculate the moving averages.

TEX<sub>86</sub> values from Site 398 prior to OAE 1a vary around 0.88. During the negative CIE TEX<sub>86</sub> values increase to a maximum of 0.95. At the onset of the

positive CIE  $\text{TEX}_{86}$  values start to decrease and reach minimum values of 0.80 during the plateau of the positive CIE (segment C7).

At Djebel Serdj only two samples contained sufficient GDGTs for SST reconstruction. Both of these samples are from isotope segment C3 with  $\text{TEX}_{86}$  values of  $\sim 0.9$ . Overall these  $\text{TEX}_{86}$  values for OAE 1a are  $\sim 0.1$ - $0.15$  units higher than those found in the modern ocean (Fig. 2c), but are similar to those reported from the subtropics during the earliest Cretaceous (Littler et al., 2011).

## DISCUSSION

SST estimates for OAE 1a using the deep time approach are overall higher than those obtained using  $\text{TEX}_{86}^{\text{H}}$ , but similar to those obtained with other linear regressions, with values at Site 398 ranging from around  $39 \pm 1$  °C pre-OAE 1a, to maximum values of 43 °C during the negative CIE, and minimum values of around 35 °C during the subsequent positive CIE (Fig. 1). Results based on the deep time approach are nearly identical to those obtained using previously published linear relationships as well as a linear relationship derived from the most up-to-date modern dataset (see SI). Although these SST estimates are higher than previous estimates based on calcite  $\delta^{18}\text{O}$ , diagenesis can artificially lower  $\delta^{18}\text{O}$  if non-pristine carbonate is used. Moreover, there is increasing evidence from new inorganic proxy records that SSTs during the Cretaceous are similar to those obtained using  $\text{TEX}_{86}$ , with tropical SSTs near 40 °C (Bice et al., 2006) as well as mid-latitude SSTs ( $\sim 40$  °N) as high as 30-36 °C (Erbacher et al., 2011). We concede that these estimated SSTs are very high and future work, using a range of proxies, is required to confirm these absolute values. We suggest, however, that the trends using the  $\text{TEX}_{86}$  deep-time analogue are

more robust than those derived from  $\text{TEX}_{86}^{\text{H}}$  that effectively shows no temporal (or spatial) variation.

It has been shown that Thaumarchaeota grown in oxygen minimum zones generate GDGTs with more cyclopentane moieties leading to a higher  $\text{TEX}_{86}$  value, in-line with culture experiments (Basse et al., 2014; Qin et al., 2015). However, this appears to have only a small impact on sedimentary  $\text{TEX}_{86}$  distributions, as values from sediments underneath oxygen minimum zones still reflect overlying SST (Basse et al., 2014). At both sites concerns regarding the potential effects of severe oxygen limitation on  $\text{TEX}_{86}$  are further mitigated by the relatively low TOC content across OAE 1a with values of around 1 wt.% and lack of biomarker evidence for photic zone euxinia in our samples. Therefore, although we do not entirely preclude the role of anoxia in generating elevated  $\text{TEX}_{86}$ -SSTs, its influence was likely minor.

#### **TEMPORAL TRENDS IN SSTs AT SITE 398**

In contrast to the  $\text{TEX}_{86}^{\text{H}}$ -based SSTs, the deep time analogue calibration results in a 2-4 °C warming during the onset of OAE 1a. SSTs start to increase at the onset of the negative  $\delta^{13}\text{C}$  excursion, and highest SST are reached after ~ 500-700 kyr during the period with the most negative  $\delta^{13}\text{C}$  values, presumably the time with highest  $p\text{CO}_2$  (Naafs et al., 2016). These results are similar to the suggested 4 °C increase in SSTs at the onset of OAE 1a found in the Atlantic boreal realm (Mutterlose et al., 2014), suggesting a basin wide forcing mechanism. A brief return to more positive  $\delta^{13}\text{C}$  values in the middle of OAE 1a is associated with lower SSTs, although based on a limited number of data points, potentially related to an episode of lower SSTs seen in other basins during C-isotope segment C4-C6 (Dumitrescu et al., 2006; Mutterlose et al., 2014).



Following a period of maximum SSTs, the onset of (two-stepped) cooling of 5-6 °C coincides with the start of the positive CIE, which is generally attributed to enhanced burial of  $^{12}\text{C}$  rich organic matter and that we interpret as a link between the enhanced burial of organic matter, drawdown of  $p\text{CO}_2$ , and SST. This cooling that took ~ 200 kyr is also recorded in SSTs from the boreal realm (Mutterlose et al., 2014) and by changes in pollen assemblages from the Tethys region that document altered rainfall patterns and a cooler climate (Hochuli et al., 1999). Unfortunately, the inability to distinguish the individual C3-C6 segments at Site 398 makes it difficult to attribute causality unambiguously, but these relationships are consistent with those frequently proposed for other CIEs.

#### **SPATIAL TRENDS IN SSTs**

Previous studies have suggested that OAE 1a was characterized by a flat/reduced latitudinal SSTs gradient (Jenkyns et al., 2012; Mutterlose et al., 2014) that is smaller than that suggested by Early Cretaceous climate model reconstructions, even when taking additional (biological) feedback mechanisms into account (e.g., Kump and Pollard, 2008). The presence of such a reduced SST gradient implies the existence of (unknown) additional high-latitude climate feedback mechanisms in a high  $p\text{CO}_2$ -world. However, those previous interpretations were based on the  $\text{TEX}_{86}^{\text{H}}$ -calibration. Recalculating all available SST-data using our linear deep time calibration yields a steeper latitudinal SST gradient, due largely to higher reconstructed tropical SSTs (Fig. 2b). This new gradient, is particularly more pronounced in the Southern Hemisphere, which is ~10-15 °C and more similar to, albeit still smaller than, the modern SST gradient.

## CONCLUSION

The response of the climate system to changes in the carbon cycle ( $p\text{CO}_2$ ) across Aptian OAE 1a is poorly constrained. Here we provide a new SST record from the mid-latitude North Atlantic across OAE 1a based on the organic geochemical  $\text{TEX}_{86}$  paleothermometer. Our results demonstrate that changes in SSTs coincided with changes in  $\delta^{13}\text{C}_{\text{org}}$  values. Although we recognise the need for caution in concluding causality, we interpret that coincidence to predominantly reflect light organic carbon release resulting in  $p\text{CO}_2$ -forced global warming, followed by organic matter sequestration and  $p\text{CO}_2$ -forced cooling. Our high tropical  $\text{TEX}_{86}$  values and resulting SSTs, higher than today, argue against the presence of a tropical thermostat and demonstrate that greenhouse climates can be associated with clear latitudinal SST gradients, more in-line with climate model simulations (Donnadieu et al., 2006). However, most climate models suggest lower absolute temperatures than those observed here and additional (multi-proxy) data is required to confirm the high absolute SSTs.

## ACKNOWLEDGEMENTS

B.D.A.N. received funding through a Rubicon fellowship, awarded by the Netherlands Organization for Scientific Research (NWO). Additional funding came from the advanced ERC grant 'The greenhouse earth system' (T-GRES, project reference 340923). R.D.P. acknowledges the Royal Society Wolfson Research Merit Award. C. O'Brien is acknowledged for discussions and help with generating the deep-time calibration.

## REFERENCES

- Ando, A., Kaiho, K., Kawahata, H., and Kakegawa, T., 2008, Timing and magnitude of early Aptian extreme warming: Unraveling primary  $\delta^{18}\text{O}$  variation in indurated pelagic carbonates at Deep Sea Drilling Project Site 463, central Pacific Ocean: *Palaeogeography, Palaeoclimatology, Palaeoecology*, v. 260, no. 3–4, p. 463-476, doi: 10.1016/j.palaeo.2007.12.007.
- Basse, A., Zhu, C., Versteegh, G. J. M., Fischer, G., Hinrichs, K.-U., and Mollenhauer, G., 2014, Distribution of intact and core tetraether lipids in water column profiles of suspended particulate matter off Cape Blanc, NW Africa: *Organic Geochemistry*, v. 72, p. 1-13, doi: 10.1016/j.orggeochem.2014.04.007.
- Bice, K. L., Birgel, D., Meyers, P. A., Dahl, K. A., Hinrichs, K.-U., and Norris, R. D., 2006, A multiple proxy and model study of Cretaceous upper ocean temperatures and atmospheric  $\text{CO}_2$  concentrations: *Paleoceanography*, v. 21, no. 2, p. PA2002, doi: 10.1029/2005pa001203.
- Bottini, C., Erba, E., Tiraboschi, D., Jenkyns, H. C., Schouten, S., and Sinninghe Damsté, J. S., 2015, Climate variability and ocean fertility during the Aptian Stage: *Climate of the Past*, v. 11, no. 3, p. 383-402, doi: 10.5194/cp-11-383-2015.
- Donnadieu, Y., Pierrehumbert, R., Jacob, R., and Fluteau, F., 2006, Modelling the primary control of paleogeography on Cretaceous climate: *Earth and Planetary Science Letters*, v. 248, no. 1–2, p. 426-437, doi: 10.1016/j.epsl.2006.06.007.
- Dumitrescu, M., Brassell, S. C., Schouten, S., Hopmans, E. C., and Sinninghe Damsté, J. S., 2006, Instability in tropical Pacific sea-surface temperatures during the early Aptian: *Geology*, v. 34, no. 10, p. 833-836, doi: 10.1130/g22882.1.
- Elling, F. J., Könneke, M., Mußmann, M., Greve, A., and Hinrichs, K.-U., 2015, Influence of temperature, pH, and salinity on membrane lipid composition and  $\text{TEX}_{86}$  of marine planktonic thaumarchaeal isolates: *Geochimica et Cosmochimica Acta*, v. 171, p. 238-255, doi: 10.1016/j.gca.2015.09.004.
- Erbacher, J., Friedrich, O., Wilson, P. A., Lehmann, J., and Weiss, W., 2011, Short-term warming events during the boreal Albian (mid-Cretaceous): *Geology*, v. 39, no. 3, p. 223-226, doi: 10.1130/G31606.1.
- Hochuli, P. A., Menegatti, A. P., Weissert, H., Riva, A., Erba, E., and Silva, I. P., 1999, Episodes of high productivity and cooling in the early Aptian Alpine Tethys: *Geology*, v. 27, no. 7, p. 657-660, doi: 10.1130/0091-7613(1999)027<0657:EOHPAC>2.3.CO;2.
- Hopmans, E. C., Weijers, J. W. H., Schefuß, E., Herfort, L., Sinninghe Damsté, J. S., and Schouten, S., 2004, A novel proxy for terrestrial organic matter in sediments based on branched and isoprenoid tetraether lipids: *Earth and Planetary Science Letters*, v. 224, no. 1-2, p. 107-116, doi: 10.1016/j.epsl.2004.05.012.
- Huguet, C., Kim, J.-H., de Lange, G. J., Sinninghe Damsté, J. S., and Schouten, S., 2009, Effects of long term oxic degradation on the  $\text{U}^{\text{K}_1}_{37}$ ,  $\text{TEX}_{86}$  and BIT organic proxies: *Organic Geochemistry*, v. 40, no. 12, p. 1188-1194, doi: 10.1016/j.orggeochem.2009.09.003.
- Jenkyns, H. C., 1995, Carbon-isotope stratigraphy and paleoceanographic significance of the lower Cretaceous shallow-water carbonates of resolution Guyot, mid-Pacific Mountains, *in* Winterer, E. L., Sager, W. W., Firth, J. V., and Sinton, J. M., eds., *Proceedings of the Ocean Drilling Program, Scientific Results*, vol. 143: College Station, TX, Ocean Drilling Program, p. 99-104.

273 Jenkyns, H. C., Schouten-Huibers, L., Schouten, S., and Sinninghe Damsté, J. S.,  
 274 2012, Warm Middle Jurassic-Early Cretaceous high-latitude sea-surface  
 275 temperatures from the Southern Ocean: *Climate of the Past*, v. 8, p. 215-226,  
 276 doi: 10.5194/cp-8-215-2012.  
 277 Kim, J.-H., van der Meer, J., Schouten, S., Helmke, P., Willmott, V., Sangiorgi, F.,  
 278 Koç, N., Hopmans, E. C., and Sinninghe Damsté, J. S., 2010, New indices and  
 279 calibrations derived from the distribution of crenarchaeal isoprenoid tetraether  
 280 lipids: Implications for past sea surface temperature reconstructions:  
 281 *Geochimica et Cosmochimica Acta*, v. 74, no. 16, p. 4639-4654, doi:  
 282 10.1016/j.gca.2010.05.027.  
 283 Kump, L. R., and Pollard, D., 2008, Amplification of Cretaceous Warmth by  
 284 Biological Cloud Feedbacks: *Science*, v. 320, no. 5873, p. 195-195, doi:  
 285 10.1126/science.1153883.  
 286 Langebroek, P., Bradshaw, C., Yanchilina, A., Caballero-Gill, R., Pew, C., Armour,  
 287 K., Lee, S.-Y., and Jansson, I.-M., 2012, Improved proxy record of past warm  
 288 climates needed: *Eos, Transactions American Geophysical Union*, v. 93, no.  
 289 14, p. 144-145, doi: 10.1029/2012EO140007.  
 290 Li, Y.-X., Bralower, T. J., Montañez, I. P., Osleger, D. A., Arthur, M. A., Bice, D. M.,  
 291 Herbert, T. D., Erba, E., and Premoli Silva, I., 2008, Toward an orbital  
 292 chronology for the early Aptian Oceanic Anoxic Event (OAE1a, ~ 120 Ma):  
 293 *Earth and Planetary Science Letters*, v. 271, no. 1-4, p. 88-100, doi:  
 294 10.1016/j.epsl.2008.03.055.  
 295 Littler, K., Robinson, S. A., Bown, P. R., Nederbragt, A. J., and Pancost, R. D., 2011,  
 296 High sea-surface temperatures during the Early Cretaceous Epoch: *Nature*  
 297 *Geoscience*, v. 4, no. 3, p. 169-172, doi: 10.1038/ngeo1081.  
 298 Menegatti, A. P., Weissert, H., Brown, R. S., Tyson, R. V., Farrimond, P., Strasser,  
 299 A., and Caron, M., 1998, High-Resolution  $\delta^{13}\text{C}$  Stratigraphy Through the  
 300 Early Aptian "Livello Selli" of the Alpine Tethys: *Paleoceanography*, v. 13,  
 301 no. 5, p. 530-545, doi: 10.1029/98pa01793.  
 302 Mutterlose, J., Bottini, C., Schouten, S., and Sinninghe Damsté, J. S., 2014, High sea-  
 303 surface temperatures during the early Aptian Oceanic Anoxic Event 1a in the  
 304 Boreal Realm: *Geology*, v. 42, no. 5, p. 439-442, doi: 10.1130/G35394.1.  
 305 Naafs, B. D. A., Castro, J. M., De Gea, G. A., Quijano, M. L., Schmidt, D. N., and  
 306 Pancost, R. D., 2016, Gradual and sustained carbon dioxide release during  
 307 Aptian Oceanic Anoxic Event 1a: *Nature Geoscience*, v. 9, no. 2, p. 135-139,  
 308 doi: 10.1038/ngeo2627.  
 309 Qin, W., Carlson, L. T., Armbrust, E. V., Devol, A. H., Moffett, J. W., Stahl, D. A.,  
 310 and Ingalls, A. E., 2015, Confounding effects of oxygen and temperature on  
 311 the TEX<sub>86</sub> signature of marine Thaumarchaeota: *Proceedings of the National*  
 312 *Academy of Sciences*, v. 112, no. 35, p. 10979-10984, doi:  
 313 10.1073/pnas.1501568112.  
 314 Ridgwell, A., 2005, A Mid Mesozoic Revolution in the regulation of ocean chemistry:  
 315 *Marine Geology*, v. 217, no. 3-4, p. 339-357, doi:  
 316 10.1016/j.margeo.2004.10.036.  
 317 Schouten, S., Forster, A., Panoto, F. E., and Sinninghe Damsté, J. S., 2007, Towards  
 318 calibration of the TEX<sub>86</sub> palaeothermometer for tropical sea surface  
 319 temperatures in ancient greenhouse worlds: *Organic Geochemistry*, v. 38, no.  
 320 9, p. 1537-1546, doi: 10.1016/j.orggeochem.2007.05.014.  
 321 Schouten, S., Hopmans, E. C., Forster, A., van Breugel, Y., Kuypers, M. M. M., and  
 322 Sinninghe Damsté, J. S., 2003, Extremely high sea-surface temperatures at

low latitudes during the middle Cretaceous as revealed by archaeal membrane lipids: *Geology*, v. 31, no. 12, p. 1069-1072, doi: 10.1130/g19876.1.

Schouten, S., Hopmans, E. C., Schefuss, E., and Sinninghe Damsté, J. S., 2002, Distributional variations in marine crenarchaeotal membrane lipids: a new tool for reconstructing ancient sea water temperatures?: *Earth and Planetary Science Letters*, v. 204, no. 1-2, p. 265-274, doi: 10.1016/S0012-821X(02)00979-2.

Taylor, K. W. R., Huber, M., Hollis, C. J., Hernandez-Sanchez, M. T., and Pancost, R. D., 2013, Re-evaluating modern and Palaeogene GDGT distributions: Implications for SST reconstructions: *Global and Planetary Change*, v. 108, p. 158-174, doi: 10.1016/j.gloplacha.2013.06.011.

Tierney, J. E., and Tingley, M. P., 2014, A Bayesian, spatially-varying calibration model for the TEX<sub>86</sub> proxy: *Geochimica et Cosmochimica Acta*, v. 127, p. 83-106, doi: 10.1016/j.gca.2013.11.026.

-, 2015, A TEX<sub>86</sub> surface sediment database and extended Bayesian calibration: *Scientific Data*, v. 2, p. 150029, doi: 10.1038/sdata.2015.29.

## FIGURE CAPTIONS

Figure 1. A)  $\delta^{13}\text{C}$  of bulk organic matter from DSDP Site 398 (Li et al., 2008) and B) TEX<sub>86</sub>-based SST using the TEX<sub>86</sub><sup>H</sup> (circles) and BAYSPAR (squares) calibrations. Stars indicate samples with BIT values between 0.41 and 0.57. Thick lines represent moving averages. Samples with BIT > 0.4 were not included in the moving average. Definition of carbon isotope segments (C2-C7), which are recognized globally, is after Li et al. (2008).

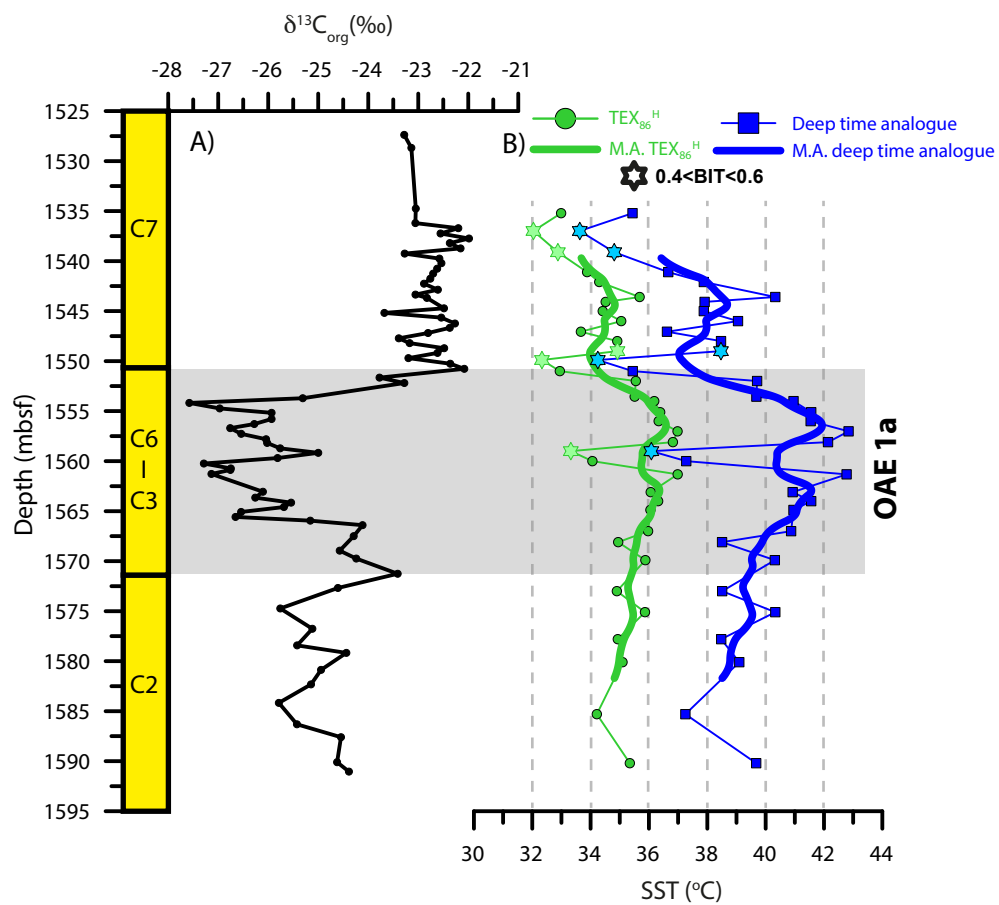
Figure 2. Modern latitudinal SST gradient (Langebroek et al., 2012) together with A) TEX<sub>86</sub><sup>H</sup> and B) BAYSPAR based SST estimates from Site 511 (Jenkyns et al., 2012), Site 463 (Schouten et al., 2003), Site 1207 (Dumitrescu et al., 2006), Site 398 (this study), Djebel Serdj (this study), and Altstätte (Mutterlose et al., 2014) across OAE 1a (carbon isotope segment C3-C6, equivalent of the Selli-level). The gradients for OAE 1a shown in A and B are the same. Error bars in A) reflect standard error of calibration of 2.5 °C, while error bars in B) represent 95% confidence intervals. C) raw TEX<sub>86</sub> values across OAE 1a together with TEX<sub>86</sub> values in modern marine core-

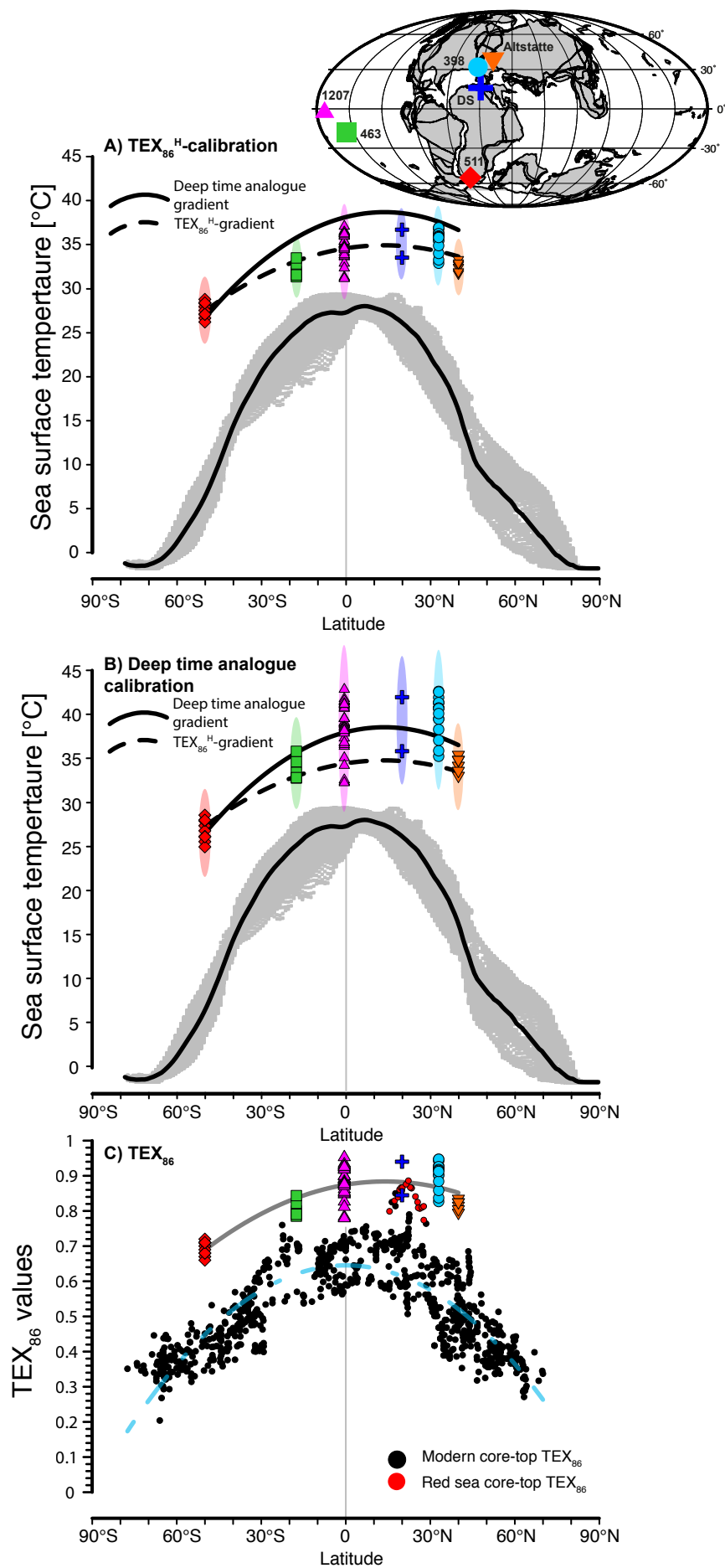
356 top sediments, excluding those from the Arctic Ocean (Tierney and Tingley, 2015).

357 Insert depicts the approximate paleogeography at 120 Myr and locations of study sites.

358

359 <sup>1</sup>GSA Data Repository item 201Xxxx, [supplementary information and data](#),







## Supplementary information Naafs and Pancost

### Detailed methods

Lipids from DSDP Site 398 were obtained by extracting 14 grams of dry sediment with an Ethos Ex microwave extraction system with a 20 ml of a mixture dicloromethane (DCM) and methanol (MeOH) (9:1, v/v). The microwave program consisted of a 10 min ramp to 70 °C (1000 W), 10 min hold at 70 °C (1000 W), and 20 min cool down. The samples from the Djebel Serdj FM in Tunisia were extracted using between 30 and 40 gram of dry sediment and Soxhlet apparatus for 24 h using DCM/MeOH (2:1 v/v). For both sample sets, copper cuttings were added to the total lipid extract (TLE) for 24 hrs to remove elemental sulphur. For Site 398 the TLE was separated into four fractions using silica (10 ml slurry) flash column chromatography and successive elution with 21 ml of hexane (Hex), 21 ml of DCM:Hex (1:1, v/v), 28 ml of DCM, and finally 14 ml of MeOH to obtain the polar fraction that contains the glycerol dialkyl glycerol tetraethers (GDGTs). For Djebel Serdj the TLE was separated into three fractions using silica (2 ml) open column chromatography and successive elution with 3 ml hexane, 4 ml hexane/DCM (3:1 v/v) and 4 ml DCM/MeOH (1:2 v/v) resulting in apolar, aromatic and polar (GDGT containing) fractions, respectively.

All samples were analyzed for their core-lipid GDGTs distribution by high performance liquid chromatography/atmospheric pressure chemical ionisation – mass spectrometry (HPLC/APCI-MS) using a ThermoFisher Scientific Accela Quantum Access triplequadrupole MS at the Organic Geochemistry Unit. Normal phase separation was achieved using two ultra-high performance liquid chromatography silica columns, following Hopmans et al. (2016). Injection volume was 15 µl, typically from 100 µl. Analyses were performed using selective ion monitoring mode (SIM) to increase sensitivity and reproducibility ( $m/z$  1302, 1300, 1298, 1296, 1294, 1292, 1050, 1048, 1046, 1036, 1034, 1032, 1022, 1020, 1018, 744, and 653). Samples were integrated manually using the Xcalibur software.

### Definition of $TEX_{86}$ and $TEX_{86}^H$ and SST calibrations over time

Schouten et al. (2002) defined  $TEX_{86}$  as a ratio of the distribution of isoprenoidal glycerol dialkyl glycerol diethers (GDGTs), archaeal membrane-spanning lipids.

$$TEX_{86} = \frac{[GDGT - 2] + [GDGT - 3] + [cren']}{[GDGT - 1] + [GDGT - 2] + [GDGT - 3] + [cren']}$$

They proposed a linear correlation between  $TEX_{86}$  and SST proxy using marine sediments from across the world (n=40).

$$TEX_{86} = 0.015 \times SST - 0.27 \quad \text{giving} \quad SST (^{\circ}C) = 66.7 \times TEX_{86} + 18$$

A linear correlation between temperature and  $TEX_{86}$  was confirmed for temperature up to 40 °C by incubation and mesocom experiments (Schouten et al., 2007; Wuchter et al., 2004).

$$TEX_{86} = 0.017 \times SST + 0.064 \quad \text{giving} \quad SST (^{\circ}C) = 58.8 \times TEX_{86} - 3.8$$

Although the intercept of this calibration differed from that found in marine core-tops, predominantly due to a difference in the amount of crenarchaeol regioisomer, the slope was comparable with that found in marine core-tops.

Kim et al. (2008) provided an updated linear calibration, based on 223 core-top samples with a global distribution.

$$TEX_{86} = 0.018 \times SST + 0.19 \quad \text{giving} \quad SST (^{\circ}C) = 56.2 \times TEX_{86} - 10.78$$

Although all previous studies used a linear correlation between  $TEX_{86}$  and temperature, including the incubation and mesocom experiments, Kim et al. (2010) proposed a logarithmic correlation between temperature and  $TEX_{86}$  for samples from core-tops with an overlying  $SST > 15^{\circ}C$ : “ $TEX_{86}^H$ ”.

$$\log(TEX_{86}) = 0.015 \times SST - 0.56 \quad \text{giving} \quad SST (^{\circ}C) = 68.4 \times \log(TEX_{86}) + 38.6$$

We note that Kim et al. (2010) also proposed an alternative ratio and calibration:  $TEX_{86}^L$ . Different from all other calibrations  $TEX_{86}^L$  is not based on the original  $TEX_{86}$  index.

$$SST (^{\circ}C) = 67.5 \times \log \left( \frac{[GDGT - 2]}{[GDGT - 1] + [GDGT - 2] + [GDGT - 3]} \right) + 46.9$$

Recently, the  $TEX_{86}^L$  approach has been vigorously critiqued because: 1) the ratio of GDGT-2 to the sum of GDGT-1, -2 and -3 has no physiological basis, unlike the original  $TEX_{86}$  ratio that records an increasing degree of cyclisation at higher temperatures (Schouten et al., 2002; Schouten et al., 2013)); 2) it has structured temperature residuals at the high end of the calibration, which is particularly problematic for its application to warm climates of the past (Tierney and Tingley, 2014); and 3) sub-surface GDGT distributions are characterized by high ratios of GDGT-2 to GDGT-3, meaning that export dynamics are particularly problematic for this proxy (Hernández-Sánchez et al., 2014; Taylor et al., 2013). As such, we do not use  $TEX_{86}^L$  here.

### Deep time analogue calibration

In order to create a deep time analogue calibration for OAE 1a we compiled all  $TEX_{86}$  records that span OAE 1a [Fig. 2](#). The deep-time model of BAYSPAR selects  $TEX_{86}$  values from the modern dataset with a similar  $TEX_{86}$  value to that of the paleorecord and then uses these locations to construct a linear regression (Tierney and Tingley, 2014). For this purpose the model requires an estimate of the prior distribution of the unknowns (basically a prediction of the SSTs to be estimated). We selected a value of  $30^{\circ}C$  and a broad standard deviation of  $20^{\circ}C$ . Selecting different values (e.g.  $25-35^{\circ}C$  as priors or smaller standard deviation) does not lead to different SSTs. The search tolerance was 0.17 ( $2\sigma$  of the inputted  $TEX_{86}$  data). The resulting linear calibration is based on “analogue” locations from the modern tropics and Red Sea.

$$TEX_{86} = 0.016 \times SST + 0.25 \quad \text{giving} \quad SST (^{\circ}C) = 60.9 \times TEX_{86} - 15.6$$

We note that much of our data fall beyond the modern calibration range, but the Bayesian approach of the BAYSPAR deep time analogue incorporates that into its error calculation.

### Linear $TEX_{86}$ calibration using all modern core tops with $SST > 15\text{ }^{\circ}\text{C}$

In addition to using the BAYSPAR deep time analogue model to create a linear calibration, we also generated a new linear  $TEX_{86}$  calibration using all modern core top data underlying surface waters with  $SST > 15\text{ }^{\circ}\text{C}$  (Fig. S1). The cut-off of  $15\text{ }^{\circ}\text{C}$  is identical to that used by  $TEX_{86}^H$ , but instead of a logarithmic correlation we use a linear correlation.

$$TEX_{86} = 0.017 \times SST + 0.22 \quad \text{giving} \quad SST\text{ (}^{\circ}\text{C)} = 58.8 \times TEX_{86} - 13.4$$

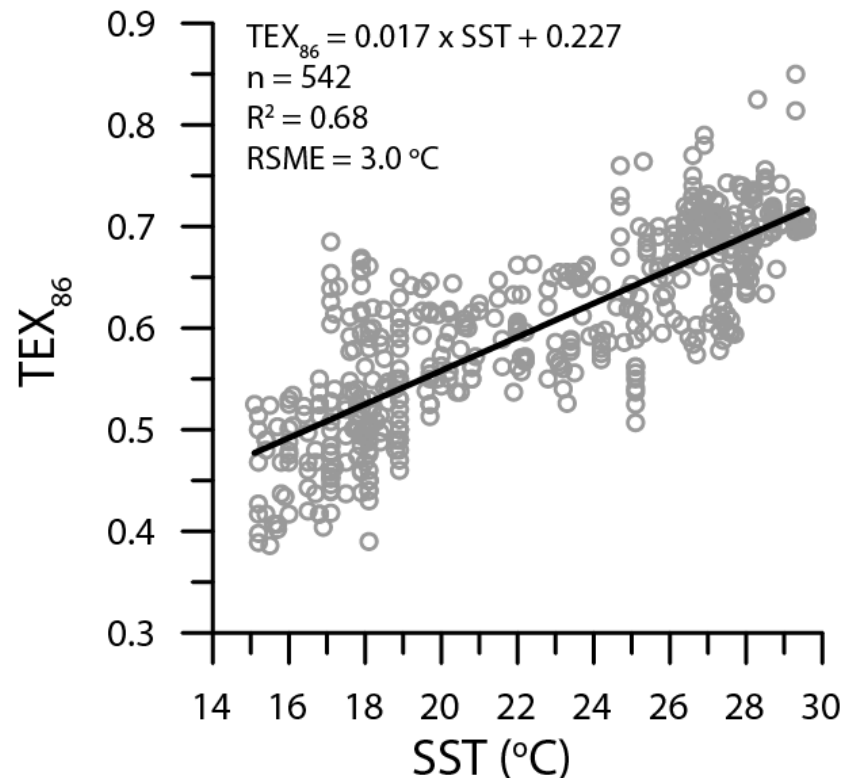


Figure S1: Newly constructed linear  $TEX_{86}$  calibration based on all core top data from regions with  $SST > 15\text{ }^{\circ}\text{C}$ . Data from Tierney and Tingley (2015)

The slope of the new linear calibration is  $\sim 60$ , virtually identical that that of the deep time analogue approach, and both of those are very similar to the slope of the high temperature calibration obtained from the incubation experiments at temperatures between  $10$  and  $40\text{ }^{\circ}\text{C}$  (Schouten et al., 2007).

Using the newly constructed calibration to generate latitudinal SST gradients for OAE 1a gives results that are nearly identical to those obtained using the BAYSPAR deep time analogue approach with a pronounced latitudinal gradient (Fig. S2). It also gives nearly identical temporal trends through OAE1a at DSDP Site 398.

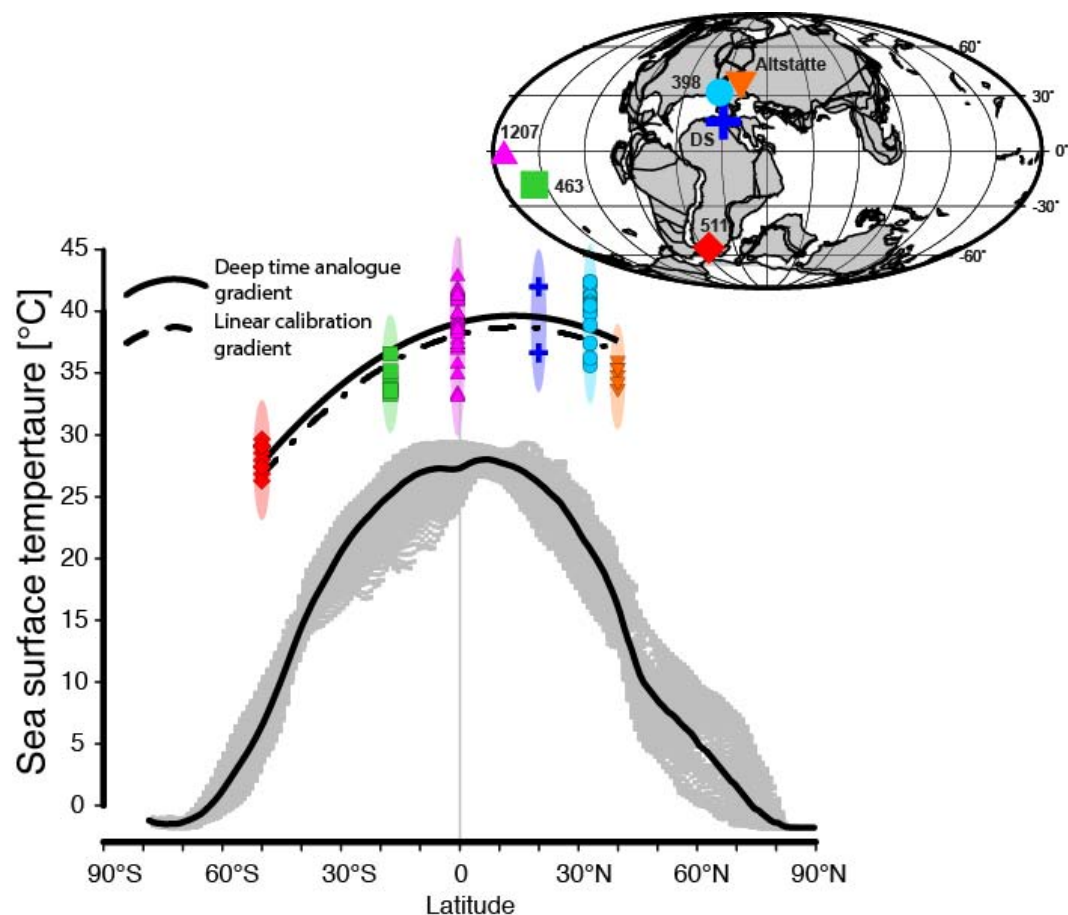


Figure S2: Latitudinal SST gradient for OAE 1a using the newly constructed linear  $TEX_{86}$  calibration, based on modern-day samples from regions with SST > 15 °C only. The deeptime analogue gradient is the same as shown in Figure 2a and b. Error bars reflect RSME of calibration, which is 3 °C.

### Supplementary references

- Hernández-Sánchez, M. T., Woodward, E. M. S., Taylor, K. W. R., Henderson, G. M., and Pancost, R. D., 2014, Variations in GDGT distributions through the water column in the South East Atlantic Ocean: *Geochimica et Cosmochimica Acta*, v. 132, p. 337-348, doi: 10.1016/j.gca.2014.02.009.
- Hopmans, E. C., Schouten, S., and Sinninghe Damsté, J. S., 2016, The effect of improved chromatography on GDGT-based palaeoproxies: *Organic Geochemistry*, v. 93, p. 1-6, doi: 10.1016/j.orggeochem.2015.12.006.
- Kim, J.-H., Schouten, S., Hopmans, E. C., Donner, B., and Sinninghe Damsté, J. S., 2008, Global sediment core-top calibration of the  $TEX_{86}$  paleothermometer in the ocean: *Geochimica et Cosmochimica Acta*, v. 72, no. 4, p. 1154-1173, doi: 10.1016/j.gca.2007.12.010.
- Kim, J.-H., van der Meer, J., Schouten, S., Helmke, P., Willmott, V., Sangiorgi, F., Koç, N., Hopmans, E. C., and Sinninghe Damsté, J. S., 2010, New indices and calibrations derived from the distribution of crenarchaeal isoprenoid tetraether lipids: Implications for past sea surface temperature reconstructions: *Geochimica et Cosmochimica Acta*, v. 74, no. 16, p. 4639-4654, doi: 10.1016/j.gca.2010.05.027.

- Schouten, S., Forster, A., Panoto, F. E., and Sinninghe Damsté, J. S., 2007, Towards calibration of the TEX<sub>86</sub> palaeothermometer for tropical sea surface temperatures in ancient greenhouse worlds: *Organic Geochemistry*, v. 38, no. 9, p. 1537-1546, doi: 10.1016/j.orggeochem.2007.05.014.
- Schouten, S., Hopmans, E. C., Schefuss, E., and Sinninghe Damsté, J. S., 2002, Distributional variations in marine crenarchaeotal membrane lipids: a new tool for reconstructing ancient sea water temperatures?: *Earth and Planetary Science Letters*, v. 204, no. 1-2, p. 265-274, doi: 10.1016/S0012-821X(02)00979-2.
- Schouten, S., Hopmans, E. C., and Sinninghe Damsté, J. S., 2013, The organic geochemistry of glycerol dialkyl glycerol tetraether lipids: A review: *Organic Geochemistry*, v. 54, p. 19-61, doi: 10.1016/j.orggeochem.2012.09.006.
- Taylor, K. W. R., Huber, M., Hollis, C. J., Hernandez-Sanchez, M. T., and Pancost, R. D., 2013, Re-evaluating modern and Palaeogene GDGT distributions: Implications for SST reconstructions: *Global and Planetary Change*, v. 108, p. 158-174, doi: 10.1016/j.gloplacha.2013.06.011.
- Tierney, J. E., and Tingley, M. P., 2014, A Bayesian, spatially-varying calibration model for the TEX<sub>86</sub> proxy: *Geochimica et Cosmochimica Acta*, v. 127, p. 83-106, doi: 10.1016/j.gca.2013.11.026.
- , 2015, A TEX<sub>86</sub> surface sediment database and extended Bayesian calibration: *Scientific Data*, v. 2, p. 150029, doi: 10.1038/sdata.2015.29.
- Wuchter, C., Schouten, S., Coolen, M. J. L., and Sinninghe Damsté, J. S., 2004, Temperature-dependent variation in the distribution of tetraether membrane lipids of marine Crenarchaeota: Implications for TEX<sub>86</sub> paleothermometry: *Paleoceanography*, v. 19, no. 4, p. PA4028, doi: 10.1029/2004PA001041.